ELSEVIER

Psychiatry Research Neuroimaging 114 (2002) 39–50

PSYCHIATRY RESEARCH NEUROIMAGING

www.elsevier.com/locate/psychresns

Changes in brain functional homogeneity in subjects with Alzheimer's disease

Nora D. Volkow[a,b,*], Wei Zhu[c], Christoph A. Felder[a], Klaus Mueller[d], Tomihisa F. Welsh[d], Gene-Jack Wang[a], Mony J. de Leon[e,f]

[a]*Medical Department, Bldg. 490, Brookhaven National Laboratory, P.O. Box 5000, Upton, NY 11973-5000, USA*
[b]*Department of Psychiatry, State University of New York, Stony Brook, NY 11794, USA*
[c]*Department of Applied Mathematics and Statistics, State University of New York, Stony Brook, NY 11794, USA*
[d]*Department of Computer Science, State University of New York, Stony Brook, NY 11794, USA*
[e]*Department of Psychiatry, New York University, New York, NY 10016, USA*
[f]*Nathan Kline Institute, Orangeburg, NY 10962, USA*

Received 9 April 2001; received in revised form 14 November 2001; accepted 28 November 2001

Abstract

Imaging studies have reported marked reductions in brain glucose metabolism in Alzheimer's Disease (AD). However, less is known about disruptions in the patterns of brain metabolic activity. Here we questioned whether AD affects the patterns of homogeneity/heterogeneity in brain metabolism. PET images of 35 AD subjects were compared with those of 35 controls. A template was applied to extract a cortical rim, which was partitioned into 990 contiguous regions. Estimates of metabolic homogeneity were obtained using the coefficient of variation (CV). The CV of the entire cortex was found to be significantly larger in AD, suggesting increased heterogeneity at the whole brain level. In contrast, regional CV was significantly lower in AD in temporal and parietal cortices, which were the regions that along with the precuneus had the largest metabolic decrements, though the precuneus had increased CV. The enhanced heterogeneity for the global cortical pattern most likely reflects variability in the degree of pathology among brain regions as well as neuroanatomical disconnection. The enhanced homogeneity in parietal and temporal cortices is likely to reflect loss of regional differentiation (i.e. macrocolumnar disorganization). The enhanced CV in precuneus, despite its marked reductions in metabolism, suggests that increases in regional homogeneity in parietal and temporal cortices are not a mere reflection of the decrement in metabolism.

Keywords: Coefficient of variation (CV); FDG; Discriminant analysis; Heterogeneity; Laterality; Positron emission tomography

1. Introduction

Imaging studies of patients with Alzheimer's Disease (AD) have consistently shown significant reductions in brain glucose metabolism, which are most accentuated in the parietotemporal cortex (Foster et al., 1984; Jagust et al., 1997; Kogure et al., 2000). The decrements in brain glucose metabolism are believed to reflect in part neuronal loss (Foster et al., 1984; Herholz, 1995). In addition to neuronal loss, histopathological studies in sub-

* Corresponding author. Tel.: +1-631-344-3335; fax: +1-631-344-5260.
E-mail address: volkow@bnl.gov (N.D. Volkow).

0925-4927/01/$ - see front matter
PII: S0925-4927(01)00130-5

jects with AD have shown a loss in the patterns of cortical connectivity (Ceccaldi et al., 1995; Desgranges et al., 1998; Giannakopoulos et al., 1995; Li et al., 2000) as well as regional columnar organization (Fonseca and Soriano, 1995; Parvizi et al., 2000; Van Hoesen and Solodkin, 1993) in part linked to amyloid deposition (Akiyama et al., 1993).

Imaging studies measuring brain glucose metabolism in AD subjects have concentrated on assessing the magnitude of the changes in regional brain metabolism while little is known about the changes in the patterns of metabolism within a given region or throughout the brain. Here we questioned whether the histopathological changes reported in AD (loss in cortical differentiation, loss of columnar organization and cortical disconnection) would lead to changes in the patterns of homogeneity/heterogeneity of brain metabolism. We hypothesized that AD subjects would have increased heterogeneity in the entire cortex due to the decreased interaction between cortical brain regions but would have enhanced homogeneity at the regional level due to loss in cortical differentiation. For this purpose we analyzed the regional brain metabolic images from a group of 35 AD patients and compared them with those of 35 controls of a similar age and equivalent gender distribution. Cortical brain regions were automatically segmented across the entire cortex and the coefficients of variations in these regions were used as the measure of regional homogeneity. In parallel, we also obtained the SPM analyses to assess if the regions with the greater changes in homogeneity were also the ones with larger metabolic decrements. The data for some of these subjects have previously been published as part of a study that compared metabolism between AD and controls (de Leon et al., 1997).

2. Methods

2.1. Subjects and clinical data

Subjects were 35 normal and 35 AD subjects with comparable age (between 60 and 85 years) and gender (20 females, 15 males) distribution (Table 1). Subjects were drawn from New York University (NYU) School of Medicine Alzheimer's Disease Center. Written informed consent was obtained from all subjects at NYU and at Brookhaven National Laboratories (BNL) (and, when appropriate, from the caregiver as well). Subjects received an extensive screening and diagnostic battery that included medical, neurologic, psychiatric, neuropsychological and neuroradiological examinations. Subjects were excluded from this study if they had evidence of a significant neurological abnormality (e.g. stroke), psychiatric disorder (e.g. depression), significant medical conditions (e.g. uncontrolled hypertension or diabetes), or sensory impairment. Both the Global Deterioration Scale (GDS) (Reisberg et al., 1982), and the Mini-Mental Status Examination (MMSE) (Folstein, 1983) were administered to stage the study participants. Subjects were categorized as follows: normal control subjects (GDS 1 or 2) and mild to severe AD patients (GDS 4–6). Furthermore, MMSE scores <27 excluded individuals from the control group. The diagnosis of AD was made according to the guidelines of the NINCDS-ADRDA criteria (McKhann et al., 1984) and DSM IV (American Psychiatric Association, 1994). Table 1 summarizes clinical characteristics of the subjects.

2.2. PET scan procedure

FDG-PET scans were obtained using a Siemens CTI-931 scanner. The scanner generates 15 axial

Table 1
Clinical characteristics of normal controls and of subjects with Alzheimer's disease

	Age	Education	GDS	MMSE
Normal subjects	71.46 ± 5.76	15.63 ± 2.39	1.83 ± 0.38	29.49 ± 0.89
AD subjects	71.34 ± 6.86	14.57 ± 2.82	4.63 ± 0.73	18.80 ± 7.89

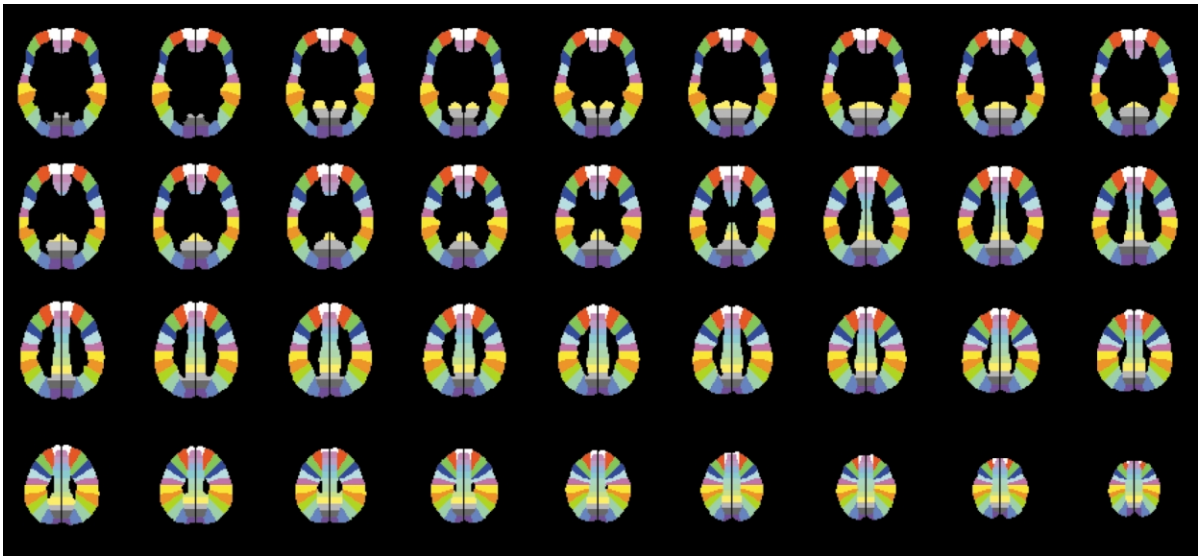

Fig. 1. Cortex partition map.

tomographic slices covering 101 mm, with nearly isotropic ~6.2–6.7 mm FWHM resolution. Each subject's head was secured with a plastic custom-molded head holder, positioned using two orthogonal laser beams, and imaged axially. Attenuation correction was obtained using a $^{68}Ga/^{68}Ge$ transmission scan. One hour prior to the PET scan, a radial artery catheter and a contralateral antecubital venous line were positioned. Subjects received 5–6 mCi of FDG intravenously. Arterial blood samples were obtained at standard intervals to monitor glucose and ^{18}F levels. During the scan subjects lay supine in the dimly lit scanner room with their eyes opened and ears unoccluded. Scanning commenced 35 min after isotope injection and lasted for 20 min. Two 10-min acquisitions are obtained. All data are decay corrected so that the amount of isotope that is recovered is corrected by the decay constant and therefore the pattern is unchanged across the two acquisitions. In order to improve the z-axis spatial resolution, we obtained and interleaved two 15-slice data acquisitions translated by one or more half slice thicknesses (~3.4 mm) (Bendriem et al., 1991). The CMRglu was calculated using standard procedures (Reivich et al., 1985).

2.3. Cortex extraction and segmentation

Each brain image was mapped to the Montréal Neurological Institute (MNI) template, which closely resembles the Talairach space, using SPM99 (Institute of Neurology, Wellcome Department of Cognitive Neurology). A cortex mask (Fig. 1) with a systematic and symmetrical partition of the cortices was created in the Talairach space and was inversely mapped back to each brain image. The outward and inward boundaries of the cortical rim were determined by using a threshold of 80 and 60%, respectively, of the whole brain metabolic mean. To ensure a uniform comparison across subjects with various brain sizes, we focused on the analysis of planes between the Talairach's vertical coordinates $z=-9$ and $z=26$. We divided this volume of the brain into 36 2-mm thick axial planes. The regions of interest (ROIs) were then extracted using an automated procedure that segmented the cortical rim into 32 angular cuts (some planes had fewer because of their anatomical structures), each with an approximately equal number of voxels (approx. 28 voxels). This partition resulted in a total of 990 ROIs.

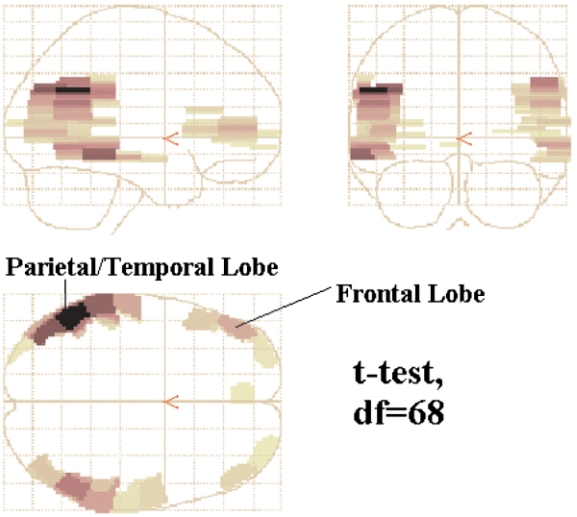

Fig. 2. Results for SPM indicating small brain regions where regional heterogeneity is significantly lower in AD than in control subjects. $\alpha = 0.05$.

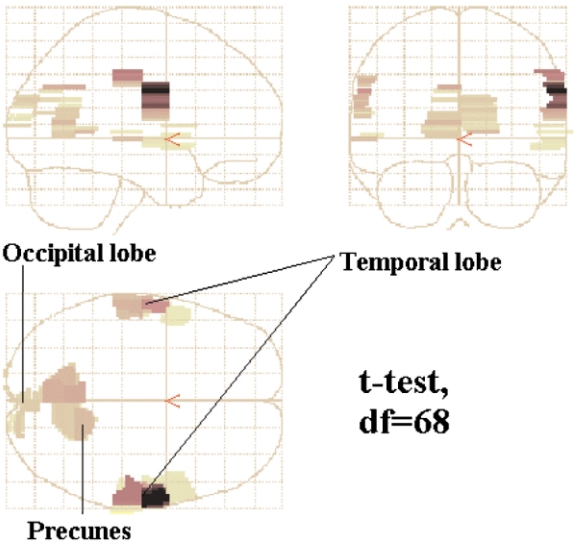

Fig. 3. Results for SPM indicating small brain regions where regional heterogeneity is significantly higher in AD than in control subjects. $\alpha = 0.05$.

2.4. Statistical procedures

2.4.1. CV

The coefficient of variation (CV), which is the ratio of the standard deviation and the mean, was adopted as the measure of heterogeneity. In this study, the CV is expressed as the percentage of the standard deviation in terms of the mean. The advantage of the CV measure lies in that it is dimensionless and unaffected by the unit/magnitude of the mean. This is particularly relevant in the metabolic image where different images are of different signal strength. The CV is also invariant to the type of metabolic measures adopted, either absolute or relative. The CV measure we proposed was calculated within each subject, both for the entire cortex (global) and for each cortical region (regional).

2.4.2. ROI-based comparison on CV, absolute and relative metabolism

Independent sample *t*-tests were performed to compare the regional heterogeneity (CV) between the controls and the AD patients on the systematically partitioned ROIs. Paired samples *t*-tests were performed to compare the heterogeneity (CV) of the corresponding left and right regional pairs. Chi-square tests for two-way contingency tables were adopted for the laterality and group comparisons. Comparisons on the metabolic means (absolute/relative) were performed similarly. The relative metabolic mean of each ROI is the ratio of the absolute metabolic mean for that ROI and the global cortical mean.

2.4.3. SPM

Relative metabolic differences between the controls and the AD patients were also examined on a voxel basis with SPM99 using the independent samples *t*-test. Statistical Parametric Maps of relative metabolic differences were displayed in coronal, transverse and sagittal views showing only voxels reaching a statistical significance of $\alpha = 0.005$ (uncorrected for multiple comparisons). Coordinates of the voxel with the highest *t*-score in each isolated significant region were reported in the Talairach and Tournoux Atlas reference space.

In order to depict the regional heterogeneity/homogeneity changes in a comparable ways for each subject, we replaced the metabolic value at each voxel with the CV value of the ROI it belonged to. These brain homogeneity images were

Table 2
Percent of ROIs for which the absolute and the relative metabolic measures and the CV were significantly higher or lower in controls than in AD subjects at $\alpha = 0.05$ for the left and the right cortex

	Absolute metabolism		Relative metabolism		CV	
	Left cortex	Right cortex	Left cortex	Right cortex	Left cortex	Right cortex
Higher	99%	98%	36%	17%	20%	8%
Lower	0%	0%	10%	15%	5%	8%

The distributions of significant CV changes in the two cortices are significantly different (χ^2 test with $P < 0.0001$).

then analyzed by SPM99 in the same way as the metabolic images. Statistical Parametric Maps of homogeneity changes were thus created and displayed in coronal, transverse and sagittal views (Figs. 2 and 3).

2.4.4. Multiple regression and discriminant analysis

To identify variables closely related to the cognitive deterioration due to AD, the best subset of variables for predicting the GDS and the MMSE were found using the SAS® REG/MAXR procedure. The two-nearest neighbor discriminant analysis was performed via the SAS® DISCRIM/NPAR procedure to examine the classification power of the metabolic mean and the CV measures. The classification rate was obtained via cross-validation (Lachenbruch and Mickey, 1968).

All *P*-values reported in this article are two-sided except those from the chi-square tests.

3. Results

3.1. Global

The global brain glucose metabolism in the segmented cortical regions was significantly lower in subjects with AD than in controls, which corresponded to 28.2 ($\pm$4.8) μmol/100 g per min and 36.9 ($\pm$4.8) μmol/100 g per min, respectively ($t = -7.58$, d.f. = 68, $P < 0.0001$). The CV across the entire cortex was significantly higher in AD than in controls and corresponded to 27.1 ($\pm$3.6) and 23.5 ($\pm$1.6), respectively ($t = 5.44$, d.f. = 68, $P < 0.0001$).

3.2. Regional measures and SPM analysis

A separate comparison for the absolute metabolic measures in the ROI showed that the reductions were significant across all cortical brain regions (Table 2). SPM analyses of the relative metabolism revealed that these reductions were most accentuated in parietal cortex, temporal cortex and precuneus (Fig. 4 and Table 3) whereas metabolism was relatively spared in motor and visual cortices as evidenced by the relative increases in those areas (Fig. 5 and Table 4). A comparison of the CV for each ROI showed greater homogeneity in AD than in controls in the left cortex. Table 2 also shows the percentage of ROIs where CV was significantly lower or higher at $\alpha = 0.05$ in AD subjects than in controls (Figs. 2 and 3 plot the anatomical locations of these regions).

In order to assess whether regions with significant changes in CV corresponded to those with

Table 3
Significant decreases in relative brain metabolism in AD subjects compared with controls

Region	Atlas coordinates				*P*-value
	x	*y*	*z*	*T*-score	
Left temporal/posterior parietal cortex	−60	−40	−12	5.21	0.001
Left temporal/posterior parietal cortex	−52	−56	12	5.40	0.001
Right temporal/posterior parietal cortex	48	−52	24	4.75	0.005
Precuneus/posterior cingulate	10	−46	28	6.32	0.000

Coordinates are from the brain atlas of Talairach and Tournoux. '*x*' is the distance in millimeters to the right (+) or left (−) of midline, '*y*' is the distance in millimeters anterior (+) or posterior (−) to the anterior commissure, and '*z*' is the distance in millimeters superior (+) or inferior (−) to a horizontal plane through the anterior and posterior commissures. *P*-values are corrected for multiple comparisons.

Table 4
Significant increases in relative brain metabolism in AD subjects as compared with findings in controls

Region	Atlas coordinates				*P*-value
	x	*y*	*z*	*T*-score	
Left motor cortex	−56	−10	24	5.93	0.000
Left putamen/pallidum	−22	−18	−4	7.30	0.000
Left visual cortex	−6	−84	4	4.95	0.002
Posterior thalamus	4	−32	−16	6.15	0.000
Right motor cortex	56	−12	24	8.08	0.000
Right putamen/pallidum	28	−18	0	8.44	0.000
Right visual cortex	14	−80	8	5.36	0.001

Coordinates are from the brain atlas of Talairach and Tournoux. '*x*' is the distance in millimeters to the right (+) or left (−) of midline, '*y*' is the distance in millimeters anterior (+) or posterior (−) to the anterior commissure, and '*z*' is the distance in millimeters superior (+) or inferior (−) to a horizontal plane through the anterior and posterior commissures. *P*-values are corrected for multiple comparisons.

the most marked changes in metabolism, we compared the maps in Figs. 2 and 3 to those in Figs. 4 and 5, where ROIs differ significantly in relative metabolism between the controls and the AD subjects, either positively or negatively, as identified by SPM. The comparison revealed that the areas with the largest metabolic decrements, which were located in parieto-temporal cortex and in precuneus, had opposite changes in regional homogeneity. The parietal association cortex (BA 39–40) was more homogeneous in AD than in controls while the opposite was true for the precuneus (BA 7), especially the left precuneus. The prefrontal cortex (BA 10) had only mild metabolic decreases, but was more homogeneous. The areas with the largest relative metabolic increases (Fig. 5), which were located in the motor cortex (BA 4 and 6) and the primary visual cortex (BA 17), were more heterogeneous.

An analysis for laterality differences in metabolism showed that in both AD and control subjects, more regions had significantly higher metabolism in the right than in the left, but this laterality effect was significantly larger for the AD patients than for the controls. The χ^2 test shows *P*-values of less than 0.0001 for both the absolute and the relative metabolism. The laterality analyses for the CV measures revealed that in controls more ROIs in the left cortex had higher CV than in the right, whereas the opposite was true for the AD subjects (Table 5). These distributions were significantly different (χ^2 test with $P<0.0001$).

3.3. Discriminant analysis

To evaluate the possible diagnostic value of CV, we performed a series of multivariate discriminant analyses (2-nearest neighbor) using the measures of absolute metabolism, and CV, for the entire cortex and for 'composite' regions generated by merging contiguous regions located either in the parietal or the precuneus area. Relative measures were not used since they did not help to further discriminate between the groups. These composite ROIs were selected since they were the regions in the SPM that differed the most in homogeneity as well as in metabolism between controls and AD subjects. The results from the discriminant analysis are summarized in Table 6.

4. Discussion

4.1. Changes in brain functional homogeneity

The regions that were more homogeneous ($\alpha = 0.05$) in AD than in controls were concentrated in three areas: the parietal and temporal association cortices and the prefrontal cortex, especially the left side. The parietal and the temporal association cortices are regions that typically show marked reductions in metabolism in AD (Herholz, 1995). The prefrontal cortex, though less consistently abnormal than the parietal-temporal cortex, also shows decrements in metabolism in AD (Foster et al., 1984). The regions that were more heteroge-

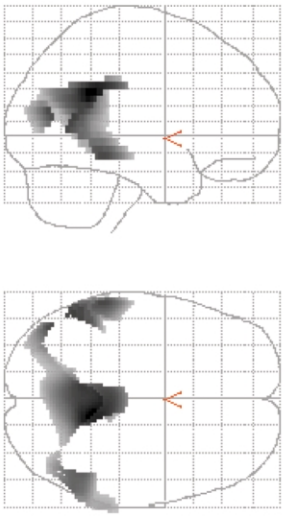

Fig. 4. Results for SPM indicating brain regions where relative metabolism was significantly lower in AD than in control subjects. $\alpha = 0.005$.

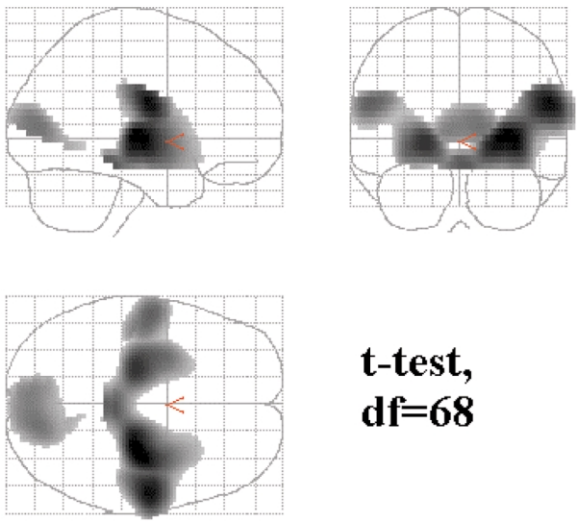

Fig. 5. Results for SPM indicating brain regions where relative metabolism was significantly higher in AD than in control subjects. $\alpha = 0.005$.

neous in AD subjects were concentrated in three areas: motor cortex, primary visual cortex, and precuneus. The motor and the primary visual cortices are usually spared by AD (Bruckner et al., 1999; Geula and Mesulam, 1996), which was evidenced in this study by the increase in their relative metabolism. In contrast, the precuneus showed a marked reduction in metabolism as the parietal association cortex but an enhanced heterogeneity in AD subjects.

We postulate that histological changes such as neuronal damage, columnar disorganization and cortical atrophy (Akiyama et al., 1993; Fonseca and Soriano, 1995; Van Hoesen and Solodkin, 1993) in AD lead to the decreased metabolism and enhanced homogeneity observed in the parietal, temporal and prefrontal ROIs. These are brain areas that show high density of neurofibrillary tangles and senile plaques in subjects and atrophy with AD (Giannakopoulos et al., 1994, 1995; Najlerahim and Bowen, 1988; Van Hoesen et al., 2000). The enhanced heterogeneity in the precuneus, which is a heterogeneous area consisting of subdivisions characterized by different cortico-cortical and cortico-thalmic connections (Andersen et al., 1987; Catalan et al., 1998; Elston et al., 1999; Salmon et al., 2000; Vanduffel et al., 1995), is likely to reflect the differential involvement of some regions but not others in AD. Functional imaging studies have shown that the precuneus is a multimodal region involved in different neural networks that are differentially affected by AD

Table 5
Percent of left/right symmetrical cortical regional pairs for which the CV and the metabolic mean (both for the absolute and the relative metabolic measures) were significantly different at $\alpha = 0.05$

	Normal controls			AD subjects		
	CV	Absolute metabolism	Relative metabolism	CV	Absolute metabolism	Relative metabolism
Left > right	6%	5%	5%	3%	0.1%	0.1%
Left < right	3%	15%	15%	8%	32%	33%

Table 6
Summary of the discriminant analysis based on CV and absolute metabolic means, in percentages

Measures	Sensitivity	Specificity	Overall
Global mean	86	86	86
Global CV	80	91	86
Global mean + global CV	94	89	91
Mean alone (global, left and right parietal, left and right precuneus)	94	94	94
CV alone (global, left and right parietal, left and right precuneus)	94	94	94
Mean (left parietal) + CV (global, left parietal, right precuneus)	94	100	97
Mean (left parietal) + CV (global, left precuneus) + age + education	100	100	100

(Backman et al., 1999; Baron et al., 2001; LaBar et al., 1999; Maddock et al., 2001; Resnick et al., 1998; Salmon et al., 2000). We speculate that differential neuronal damage and disconnection of its subdivisions might have caused a mosaicked appearance in this region that resulted in the enhanced heterogeneity.

Overall, the results on the CV are dependent on the level of ROI analyses. When the analysis is done on the entire cortex, the brains of AD subjects show greater CV than those of controls, whereas on the regional level they tend to show lower CV. The increased homogeneity on the regional level, as discussed previously, could result from AD-related histological changes. The enhanced CV in the entire cortex, on the other hand, is likely to reflect several processes that result in heterogeneity at the macro-anatomical level (Arendt et al., 1998; Giannakopoulos et al., 1995; Narisawa-Saito et al., 1996; Shukla and Bridges, 1999). These include disconnections between brain regions as well as the variability across brain regions in the magnitude of the metabolic and structural changes that lead to some brain regions having marked reductions in metabolism and atrophy (parietal cortex) while others are left relatively intact (motor cortex). Alternatively, one could argue that the increased homogeneity in the brain regions maximally affected by AD could simply be a floor effect. In contrast, the increased heterogeneity in the brain regions characteristically unaffected by AD could result from the topographical heterogeneity of the disease.

4.2. Laterality

The left cortex was more affected than the right in AD subjects as evidenced by the larger decrements in absolute and relative metabolism as well as the larger number of ROIs that were more homogeneous in the left than in the right cortex. A predominance of left abnormalities in AD subjects had previously been reported in postmortem studies (Li et al., 2000), MR/CT brain volume measures (Savolainen et al., 2000; Ueyama et al., 1994), brain bioelectrical activity studies (Alvarez et al., 1999), right-side neglect (Bartolomeo et al., 1998), and PET metabolic measurements (Desgranges et al., 1998). Moreover, left-sided deficits were shown to be more predictive of cognitive decline in AD than those in the right cortex (Keilp et al., 1996). The global CV of the left cortex alone is significantly correlated with both GDS ($r=0.37$, $P=0.03$) and MMSE ($r=-0.38$, $P=0.03$), while the CV of the right cortex is not.

For the normal controls the cortex is more homogeneous on the right than the left and the right side is also more active metabolically than the left. This could reflect the postulate that the right brain is in charge of processing novel stimuli and therefore, has to be more flexible than the left cortex, which is more differentiated (Tucker and Williamson, 1984). In contrast, for the AD patients the left cortex is more homogeneous than the right, which is concordant with a greater involvement of the left cortex than of the right in AD.

4.3. Discriminant analysis

The average MMSE score for our AD group is 18, and clinically it is not difficult to differentiate an AD patient with a MMSE score of 18 from a normal elderly person. However, the AD subjects in our study are of differential disease severity with MMSE scores ranging from 2 to 30. Sixty

percent of our AD subjects have MMSE scores more than 18, 26% have scores of at least 25 and 11% of at least 28; while 14% of our control subjects have MMSE scores of no more than 28, with the maximum score for either group being 30. Thus, at an individual level it is not always easy to differentiate between the subjects with mild AD and the elderly subjects with borderline MMSE scores.

Discriminant analyses based on levels of brain glucose metabolism have been done previously (Jelic et al., 1999; Jobst et al., 1994); however, this is the first time that the homogeneity measure (CV) has been included. An intensive search of published literature revealed that the best performance in discrimination between AD and the normal subjects is attained by using the 3D stereotaxic surface projections from the metabolic images (Minoshima et al., 1995). It involved the normalized *z*-score of each voxel in the parietal association cortex plus its stereotactic coordinates and metabolic indices derived from the unilaterally averaged parietal-temporal-frontal cortex. It showed a sensitivity of 97% with a specificity of 100%. This agrees extremely well with our results of 94% sensitivity and 100% specificity achieved by a combination of the mean and CV measures from the entire cortex as well as the parietal and precuneus ROIs. The 3D discrimination is superior to other discriminant analyses based on regional and global metabolism alone, which might be the result of its utilization of the 3D metabolic distribution of the entire parietal association cortex and the unilaterally condensed distribution of the parietal-temporal-frontal cortex. CV helped summarize this distributional information in terms of the regional metabolic variation, and thus, compensated for the limitation of the average metabolic measures alone.

4.4. SPM and changes in relative metabolism

In this study the results from the SPM analyses revealed that the largest decrements were in the precuneus, posterior cingulate and posterior parietal temporal cortex. These results are almost identical to those previously reported (Desgranges et al., 1998; Kogure et al., 2000; Ishii et al., 1997).

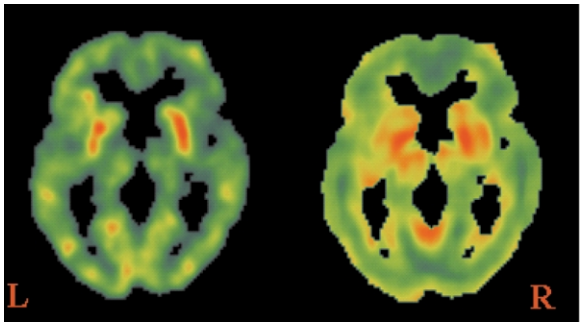

Fig. 6. PET metabolic image (L) and the local CV map (R).

This high degree of replicability emphasizes the consistency of the pattern of metabolic abnormalities seen in subjects with AD. The SPM maps also showed that the subjects with AD had 'relative' increases in the primary visual cortex, motor cortex, basal ganglia and posterior thalamus. Since these differences were obtained after normalization for global metabolism, these 'relative increases' are usually regarded as reflecting relative sparing of these brain regions by AD.

4.5. Limitations and on-going work

The regional homogeneity measure (CV) is a new parameter to describe metabolic changes in the brain. We cannot ascertain the ranges that are considered to be normal and the extent to which these ranges will vary as a function of the mental state of the subjects and the conditions under which the studies were performed. Future studies evaluating changes in CV between controls and AD subjects during activation conditions would provide further information on the responsiveness of the AD brain to activation beyond just an analysis of the magnitude of changes in glucose utilization.

The CV map where the metabolic value at each voxel is replaced by the corresponding regional CV is not smooth. Thus, the SPM analysis on CV presented here is of an exploratory nature: one can examine regions that are significantly different in homogeneity between the groups via the SPM *t*-tests; however, one cannot utilize the results based on the random field theory (the cluster or set level

P-values), which requires the smoothness assumption. In parallel, we have been developing the local CV method where the CV value of each voxel is obtained based on its small neighborhood (Fig. 6). The CV map obtained in this way is smooth. We could also avoid the selection of pre-defined ROIs. However, the local CV is dependent upon the neighborhood size. More studies are needed to gain experience with and understanding of this new approach.

We also point out that the lack of atrophy correction due to the lack of MR images could potentially influence the results. Previous study (Ibanez et al., 1998) demonstrated that the regional metabolic mean is robust to atrophy correction — regions with significant difference between AD and normal controls are consistent before and after atrophy correction. However, the influence of atrophy on brain homogeneity has yet to be examined.

In conclusion, this study confirms the previous findings of reductions in metabolism in AD subjects, which are most accentuated in posterior cingulate, parieto-temporal cortex, precuneus and left cortex. It also revealed a marked disruption in the patterns of homogeneity as evidenced by an increase in homogeneity in parietal and prefrontal cortex and an increase in heterogeneity in the whole cortex and in precuneus. We postulate that neuronal damage, columnar disorganization and cortical atrophy lead to the enhanced homogeneity observed in the parietal and prefrontal cortex whereas disconnection from white matter lesions and the mosaic of differentially affected brain regions lead to the increased heterogeneity in the whole cortex. The mechanism underlying the enhanced heterogeneity in the precuneus, an area with marked reduction in metabolism, is unclear and requires further investigation. Also the contribution of brain atrophy to the CV measures needs to be evaluated.

Acknowledgments

This work was funded in part by grants from the NIH-NIA (AG13616, AG12101, AG03051, AG08051) (NYU) and by DOE (OBER). We thank the editor and the three referees who have provided many insightful comments and suggestions that have greatly clarified and improved our work.

References

Akiyama, H., Yamada, T., McGeer, P.L., Kawamata, T., Ooyama, I., Ishii, T., 1993. Columnar arrangement of beta-amyloid protein deposits in the cerebral cortex of patients with Alzheimer's disease. Acta Neuropathologica 85, 400–403.

Alvarez, X.A., Mouzo, R., Pichel, V., Perez, P., Laredo, M., Fernandez-Novoa, E., Corzo, L., Zas, R., Alcaraz, M., Secades, J.J., Lozano, R., Cacabelos, R., 1999. Double-blind placebo-controlled study with citicoline in APOE genotyped Alzheimer's disease patients. Effects on cognitive performance, brain bioelectrical activity and cerebral perfusion. Methods and Findings in Experimental and Clinical Pharmacology 21, 633–644.

American Psychiatric Association, 1994. Diagnostic and Statistical Manual of Mental Disorders (Fourth Edition), American Psychiatric Press, Washington, D.C.

Andersen, R.A., Essick, G.K., Siegel, R.M., 1987. Neurons of area 7 activated by both visual stimuli and oculomotor behavior. Experimental Brain Research 67, 316–322.

Arendt, T., Bruckner, M.K., Gertz, H.J., Marcova, L., 1998. Cortical distribution of neurofibrillary tangles in Alzheimer's disease matches the pattern of neurons that retain their capacity of plastic remodeling in the adult brain. Neuroscience 83, 991–1002.

Backman, L., Andersson, J.L., Nyberg, L., Winblad, B., Nordberg, A., Almkvist, O., 1999. Brain regions associated with episodic retrieval in normal aging and Alzheimer's disease. Neurology 52, 1861–1870.

Baron, J.C., Chetelat, G., Desgranges, B., Perchey, G., Landeau, B., de la Sayette, V., Eustache, F., 2001. In vivo mapping of gray matter loss with voxel-based morphometry in mild Alzheimer's disease. Neuroimage 14, 298–309.

Bartolomeo, P., Dalla Barba, G., Boisse, M.F., Bachoud-Levi, A.C., Degos, J.D., Boller, F., 1998. Right-side neglect in Alzheimer's disease. Neurology 51, 1207–1209.

Bendriem, B., Dewey, S.L., Schlyer, D.J., Wolf, A.P., Volkow, N.D., 1991. Quantitation of the human basal ganglia with positron emission tomography: a phantom study of the effect of contrast and axial positioning. IEEE Transactions on Nuclear Science 10, 216–222.

Bruckner, G., Hausen, D., Hartig, W., Drlicek, M., Arendt, T., Brauer, K., 1999. Cortical areas abundant in extracellular matrix chondroitin sulfate proteoglycans are less affected by cytoskeletal changes in Alzheimer's disease. Neuroscience 92, 791–805.

Catalan, M.J., Honda, M., Weeks, R.A., Cohen, L.G., Hallett, M., 1998. The functional neuroanatomy of simple and complex sequential finger movements: a PET study. Brain 121, 253–264.

Ceccaldi, M., Poncet, M., Gambarelli, D., Guinot, H., Bille, J., 1995. Progressive severity of left unilateral apraxia in 2 cases of Alzheimer disease. Revue Neurologique 151, 240–246.

de Leon, M.J., McRae, T., Rusinek, H., Convit, A., De Santi, S., Tarshish, C., Golomb, J., Volkow, N., Daisley, K., Orentreich, N., McEwen, B., 1997. Cortisol reduces hippocampal glucose metabolism in normal elderly but not in Alzheimer's disease. Journal of Clinical Endocrinology and Metabolism 82, 3251–3259.

Desgranges, B., Baron, J.C., de la Sayette, V., Petit-Taboué, M.C., Benali, K., Landeau, B., Lechevalier, B., Eustache, F., 1998. The neural substrates of memory systems impairment in Alzheimer's disease. A PET study of resting brain glucose utilization. Brain 121, 611–631.

Elston, G.N., Tweedale, R., Rosa, M.G.P., 1999. Supragranular pyramidal neurons in the medial posterior parietal cortex of the macaque monkey: morphological heterogeneity in subdivisions of area 7. NeuroReport 10, 1925–1929.

Folstein, M., 1983. The Mini-Mental State Examination. In: Crook, T., Ferris, S.H., Bartus, R. (Eds.), Assessment in Geriatric Psychopharmacology, Mark Powley Associates, New Canaan, CT, . pp. 47–51.

Fonseca, M., Soriano, E., 1995. Calretinin-immunoreactive neurons in the normal human temporal cortex and in Alzheimer's disease. Brain Research 691, 83–91.

Foster, N.L., Chase, T.N., Mansi, L., Brooks, R., Fedio, P., Patronas, N.J., Di Chiro, G., 1984. Cortical abnormalities in Alzheimer's disease. Annals of Neurology 16, 649–654.

Geula, C., Mesulam, M.M., 1996. Systematic regional variations in the loss of cortical cholinergic fibers in Alzheimer's disease. Cerebral Cortex 6, 165–177.

Giannakopoulos, P., Hof, P.R., Bouras, C., 1994. Alzheimer's disease with asymmetric atrophy of the cerebral hemispheres: morphometric analysis of 4 cases. Acta Neuropathologica 88, 440–447.

Giannakopoulos, P., Hof, P.R., Giannakopoulos, A.S., Herrmann, F.R., Michel, J.P., Bouras, C., 1995. Regional distribution of neurofibrillary tangles and senile plaques in the cerebral cortex of very old patients. Archives of Neurology 52, 1150–1159.

Herholz, K., 1995. FDG PET and differential diagnosis of dementia. Alzheimer Disease and Associated Disorders 9, 6–16.

Ibanez, V., Pietrini, P., Alexander, G.E., Furey, M.L., Teichberg, D., Rajapakse, J.C., Rapoport, S.I., Schapiro, M.B., Horwitz, B., 1998. Regional glucose metabolic abnormalities are not the result of atrophy in Alzheimer's disease. Neurology 50, 1585–1593.

Ishii, K., Sasaki, M., Yamaji, S., Sakamoto, S., Kitagaki, H., Mori, E., 1997. Demonstration of decreased posterior cingulate perfusion in mild Alzheimer's disease by means of $H_2^{15}O$ positron emission tomography. European Journal of Nuclear Medicine 24, 670–673.

Jagust, W.J., Eberling, J.L., Reed, B.R., Mathis, C.A., Budinger, T.F., 1997. Clinical studies of cerebral blood flow in Alzheimer's disease. Annals of the New York Academy of Science 26, 254–262.

Jelic, V., Wahlund, L.O., Almkvist, O., Johansson, S.E., Shigeta, M., Winblad, B., Nordberg, A., 1999. Diagnostic accuracies of quantitative EEG and PET in mild Alzheimer's disease. Alzheimers Reports 2, 291–298.

Jobst, K.A., Hindley, N.J., King, E., Smith, A.D., 1994. The diagnosis of Alzheimer's disease — a question of image. Journal of Clinical Psychiatry 55, 22–31.

Keilp, J.G., Alexander, G.E., Stern, Y., Prohovnik, I., 1996. Inferior parietal perfusion, lateralization, and neuropsychological dysfunction in Alzheimer's disease. Brain and Cognition 32, 365–383.

Kogure, D., Matsuda, H., Ohnishi, T., Asada, T., Uno, M., Kunihiro, T., Nakano, S., Takasaki, M., 2000. Longitudinal evaluation of early Alzheimer's disease using brain perfusion SPECT. Journal of Nuclear Medicine 41, 1155–1162.

Lachenbruch, P.A., Mickey, M.A., 1968. Estimation of error rates in discriminant analysis. Technometrics 10, 1–10.

LaBar, K.S., Gitelman, D.R., Parrish, T.B., Mesulam, M., 1999. Neuroanatomic overlap of working memory and spatial attention networks: a functional MRI comparison within subjects. Neuroimage 10, 695–704.

Li, F., Iseki, E., Kato, M., Adachi, Y., Akagi, M., Kosaka, K., 2000. An autopsy case of Alzheimer's disease presenting with primary progressive aphasia: a clinicopathological and immunohistochemical study. Neuropathology 20, 239–245.

Maddock, R.J., Garrett, A.S., Buonocore, M.H., 2001. Remembering familiar people: the posterior cingulate cortex and autobiographical memory retrieval. Neuroscience 104, 667–676.

McKhann, G., Drachman, D., Folstein, M., Katzman, R., Price, D., Stadlan, E.M., 1984. Clinical diagnosis of Alzheimer's disease: report of the NINCDS-ADRDA work group under the auspices of Department of Health and Human Services Task Force on Alzheimer's disease. Neurology 34, 939–944.

Minoshima, S., Frey, K.A., Koeppe, R.A., Foster, N.L., Kuhl, D.E., 1995. A diagnostic-approach in Alzheimer's disease using 3-dimensional stereotaxic surface projections of fluorine-18-FDG PET. Journal of Nuclear Medicine 36, 1238–1248.

Najlerahim, A., Bowen, D.M., 1988. Regional weight loss of the cerebral cortex and some subcortical nuclei in senile dementia of the Alzheimer type. Acta Neuropathologica 75, 509–512.

Narisawa-Saito, M., Wakabayashi, K., Tsuji, S., Takahashi, H., Nawa, H., 1996. Regional specificity of alterations in NGF, BDNF and NT-3 levels in Alzheimer's disease. Neuroreport 7, 2925–2928.

Parvizi, J., Van Hoesen, G.W., Damasio, A., 2000. Selective pathological changes of the periaqueductal gray matter in Alzheimer's disease. Annals of Neurology 2000, 344–353.

Reisberg, B., Ferris, S.H., de Leon, M.J., Crook, T., 1982. The global deterioration scale for assessment of primary degenerative dementia. American Journal of Psychiatry 139, 1136–1139.

Reivich, M., Alavi, A., Wolf, A., Fowler, J., Russell, J., Arnett, C., MacGregor, R.R., Shiue, C.Y., Atkins, A., Anand, A.,

1985. Glucose metabolic rate kinetic model parameter determination in humans: the lumped constants and rate constants for [^{18}F]fluorodeoxyglucose and [^{11}C]deoxyglucose. Journal of Cerebral Blood Flow and Metabolism 5, 179–192.

Resnick, S.M., Maki, P.M., Golski, S., Kraut, M.A., Zonderman, A.B., 1998. Effects of estrogen replacement therapy on PET cerebral blood flow and neuropsychological performance. Hormones and Behavior 34, 171–182.

Salmon, E., Collette, F., Degueldre, C., Lemaire, C., Franck, G., 2000. Voxel-based analysis of confounding effects of age and dementia severity on cerebral metabolism in Alzheimer's disease. Human Brain Mapping 10, 39–48.

Savolainen, S., Laakso, M.P., Paljarvi, L., Alafuzoff, I., Hurskainen, H., Partanen, K., Soininen, H., Vapalahti, M., 2000. MR imaging of the hippocampus in normal pressure hydrocephalus: correlations with cortical Alzheimer's disease confirmed by pathologic analysis. American Journal of Neuroradiology 21, 409–414.

Shukla, C., Bridges, L.R., 1999. Regional distribution of tau, beta-amyloid and beta-amyloid precursor protein in the Alzheimer's brain: a quantitative immunolabeling study. Neuroreport 10, 3785–3789.

SPM99. Institute of Neurology, Wellcome Department of Cognitive Neurology.

Tucker, D.M., Williamson, P.A., 1984. Asymmetric neural control systems in human self-regulation. Psychological Review 91, 185–215.

Ueyama, K., Fukuzako, H., Fukuzako, T., Hokazono, Y., Takeuchi, K., Hashiguchi, T., Takigawa, M., Yamanaka, T., Matsumoto, K., 1994. CT study in senile dementia of Alzheimer type. International Journal of Geriatric Psychiatry 9, 919–924.

Vanduffel, W., Vandenbussche, E., Singer, W., Orban, G.A., 1995. Metabolic mapping of visual areas in the behaving cat: a [^{14}C]2-deoxyglucose study. Journal of Comparative Neurology 354, 161–180.

Van Hoesen, G.W., Solodkin, A., 1993. Some modular features of temporal cortex in humans as revealed by pathological-changes in Alzheimer's disease. Cerebral Cortex 3, 465–475.

Van Hoesen, G.W., Parvizi, J., Chu, C.C., 2000. Orbitofrontal cortex pathology in Alzheimer's disease. Cerebral Cortex 10, 243–251.